ChemComm

COMMUNICATION

View Article Online
View Journal | View Issue

Cite this: *Chem. Commun.*, 2024, **60**, 10756

Received 7th July 2024,
Accepted 12th August 2024

DOI: 10.1039/d4cc03388d

rsc.li/chemcomm

Controlling and predicting alkyl-onium electronic structure†

Frances K. Towers Tompkins,[a] Lewis G. Parker,[a] Richard M. Fogarty,[b] Jake M. Seymour,[a] Ekaterina Gousseva,[a] David C. Grinter,[c] Robert G. Palgrave,[d] Christopher D. Smith,[a] Roger A. Bennett,[a] Richard P. Matthews *[e] and Kevin R. J. Lovelock *[a]

X-ray photoelectron spectroscopy (XPS) and *ab initio* calculations show that fully alkylated onium cation electronic structure can be tuned using both the alkyl chains and the central onium atom. The key for tuning the central onium atom is methyl *versus* longer alkyl chains, allowing selection of the optimum cation for a wide range of applications, including catalysis and biocides.

Fully alkylated onium cations feature in a wide range of applications,[1] including organic synthesis,[2–4] biocides,[5,6] electrochemical energy storage materials,[7,8] friction/corrosion additives,[9,10] and solar energy capture/storage materials.[11] Two key structural variations of alkylated oniums are: (i) alkyl substituents, C_nH_{2n+1}, *e.g.* from four CH_3 in tetramethylammonium ($[N_{1,1,1,1}]^+$), to much longer alkyls; (ii) central X atom *e.g.* tetraalkylammonium ($[N_{n,n,n,n}]^+$), trialkylsulfonium ($[S_{n,n,n}]^+$) or tetraalkylphosphonium ($[P_{n,n,n,n}]^+$) (Fig. 1). This structural variation gives the potential to finely tune properties and performance,[8] although the focus has been on using the cation alkyl chain to control hydrophobicity or steric interactions.

Electrostatic interactions are key for onium–anion and onium–neutral molecule interactions, as there are no π-bonds and only σ-bonds on fully alkylated onium cations. In synthesis, hydrogen bonding catalysis is based on electrostatic interactions between onium cations and substrates,[2,3] and phase-transfer catalysis relies on anion–onium cation electrostatic interactions.[4] For biocides the first stage of $[N_{n,n,n,n}]^+$ interaction with a cell membrane is *via* an electrostatic interaction between the positively charged $[N_{n,n,n,n}]^+$ headgroup and anionic parts of the membrane.[5,6,12–15] Moreover, a single calculable electronic descriptor that can capture through-bond effects has been used to understand the impact of substituents on $[N_{n,n,n,n}]^+$,[16,17] and a range of calculated electronic structure properties (*e.g.* orbital energies) have been used to predict the impact of $[N_{n,n,n,n}]^+$ supporting electrolytes on electrochemical performance.[8] Despite these extensive examples, there is still a large knowledge gap in the electronic structure of fully alkylated onium cations that underpins electrostatic interactions in the wide variety of applications. Using a combination of experimental X-ray photoelectron spectroscopy (XPS) and lone-ion-SMD (solvation model based on density) density functional theory (DFT) calculations we provide both experimental and computational evidence on liquid-phase onium cations.

Element-specific XPS core-level binding energies, E_B(core), are capable of capturing multiple electronic structure descriptors for each onium cation, *e.g.* E_B(N 1s) and E_B(C 1s). Moreover, E_B(core) and the electrostatic potential at a nucleus, V_n, have been found to be linearly correlated for ionic liquids (ILs),[18,19] meaning that E_B(core) can be readily interpreted unlike *e.g.* chemical shifts in NMR. Furthermore, V_n is an excellent localised non-covalent bonding/reactivity strength descriptor;[20] atoms with large E_B(core) and large V_n will attract electrons relative to atoms with small E_B(core) and small V_n.

ILs with relatively weakly interacting anions, *e.g.* $[NTf_2]^-$ (bis[(trifluoromethane)sulfonyl]imide) or $[FSI]^-$ (bis(fluorosulfonyl)imide), can be used to probe intrinsic cation properties, as cations are effectively in a sea of anions that give non-specific interactions.[18,19] Additionally, lone-cation-SMD calculations (*i.e.* with no counteranions) capture the inherent cation properties.

[a] *Department of Chemistry, University of Reading, UK. E-mail: k.r.j.lovelock@reading.ac.uk*
[b] *Department of Chemistry, Imperial College London, UK*
[c] *Diamond Light Source, UK*
[d] *Department of Chemistry, University College London, UK*
[e] *Department of Biosciences, University of East London, UK. E-mail: RMatthews3@uel.ac.uk*

† Electronic supplementary information (ESI) available. See DOI: https://doi.org/10.1039/d4cc03388d

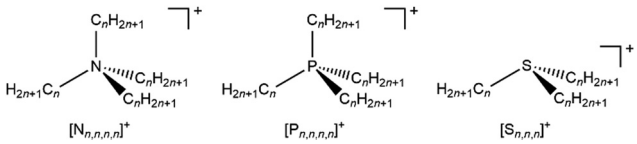

Fig. 1 Fully alkylated onium cation structures (see ESI,† Section S3 for cations studied).

The range of onium cations studied in the liquid-phase using XPS to date is limited, with the main focus on onium cations in ILs[21–25] (ILs have sufficiently low vapour pressure to be used with standard XPS apparatus[26]). A key finding for XPS of $[N_{n,n,n,n}]^+$-based ILs was the impact of cations with linear (*e.g.* $[N_{6,6,6,14}]^+$ ammonium cation) *versus* ring (*e.g.* $[C_8C_1Pyrr]^+$ pyrrolidinium cation) alkyl on the IL electronic structure; cation–anion interactions were linked to the conformational flexibility of the cation.[22,23] However, the number of different onium cations studied was relatively limited, leaving open questions, *e.g.* what is the influence of the alkyl substituent on onium electronic structure? Herein, we measured E_B(core) for 12 [onium cation][NTf_2] and two [onium cation][FSI] ILs using XPS and performed lone-ion-SMD DFT calculations (ESI† Section S3) for 31 onium cations to address these questions.

Varying the alkyl chain length of $[N_{n,n,n,n}]^+$ from methyl to longer has a significant and predictable impact on $E_B(N_{cation}\ 1s)$. N 1s XPS for the two ILs $[N_{4,1,1,1}][NTf_2]$ and $[N_{4,2,2,2}][NTf_2]$ gave a relatively large $\Delta E_B(N_{cation}\ 1s)$ of −0.36 eV (Fig. 2a and 3a and ESI,† Table S8), representing $\Delta E_B(N_{cation}\ 1s)$ going from three CH_3 to three longer alkyl chains. Each successive change of one CH_3 to one longer alkyl gives $\Delta E_B(N_{cation}\ 1s)$ of ∼−0.12 eV (Fig. 2a), as demonstrated by $\Delta E_B(N_{cation}\ 1s)$ from $[N_{4,1,1,1}][NTf_2]$ to $[N_{3,2,1,1}][NTf_2]$ to $[N_{4,4,4,1}][NTf_2]$ to $[N_{4,2,2,2}][NTf_2]$ (Fig. 2a and 3a and ESI,† Table S8). This effect of the alkyl chain lengths on cation electronic structure is independent of the anion identity, as the same $\Delta E_B(N_{cation}\ 1s)$ effect is observed when the $[FSI]^-$ anion was used, *e.g.* $[N_{4,4,4,1}][FSI]$ *versus* $[N_{4,1,1,1}][FSI]$ (ESI,† Fig. S17 and Table S8).

Changing the alkyl substituent from ethyl to longer had no discernible impact on $E_B(N_{cation}\ 1s)$, with clear evidence from three cases: (i) $[N_{n,1,1,1}]^+$ (where n = 3, 4 and 6) gave the same $E_B(N_{cation}\ 1s)$; (ii) $[N_{n,2,2,2}]^+$ (where n = 4 and 8) gave the same $E_B(N_{cation}\ 1s)$; (iii) $[N_{4,4,4,1}]^+$ and $[N_{8,8,8,1}]^+$ gave the same $E_B(N_{cation}\ 1s)$ (Fig. 2a and ESI,† Table S8).

Linear *versus* large ring alkyl chains, *e.g.* ammonium *versus* pyrrolidinium, had no discernible impact on experimental $E_B(N_{cation}\ 1s)$. Cations with one CH_3 substituent and either all linear longer alkyl chains ($[N_{4,4,4,1}][NTf_2]$, $[N_{8,8,8,1}][NTf_2]$) or large ring alkyl chains ($[C_4C_1Pip][NTf_2]$, $[C_8C_1Pyrr][NTf_2]$) gave the same $E_B(N_{cation}\ 1s)$ within experimental uncertainty (Fig. 2a and ESI,† Table S8).

Calculated $E_B(N_{cation}\ 1s)$ match experimental $E_B(N_{cation}\ 1s)$ very well, both visually (Fig. 2a and b and ESI,† Fig. S18) and an excellent linear correlation (ESI,† Fig. S20). Going from $[N_{1,1,1,1}]^+$ to $[N_{2,2,2,2}]^+$, each time a CH_3 is changed to a longer alkyl chain gives $\Delta E_B(N_{cation}\ 1s)$ ∼−0.08 eV (Fig. 2b and 3a), which is slightly smaller than the experimental $\Delta E_B(N_{cation}\ 1s)$ of ∼−0.12 eV. This difference may arise from the choice of functional/basis set combinations; the wB97XD functional was selected as it has minimal self-interaction error and correctly describes long-range electron–electron interactions (important in determining ionisation energies). An alternative explanation is the failure of the SMD model to capture local interactions (switching from IL SMD to water SMD had a small impact on $\Delta E_B(N_{cation}\ 1s)$, Fig. S19c, S19d and Table S9, ESI†).

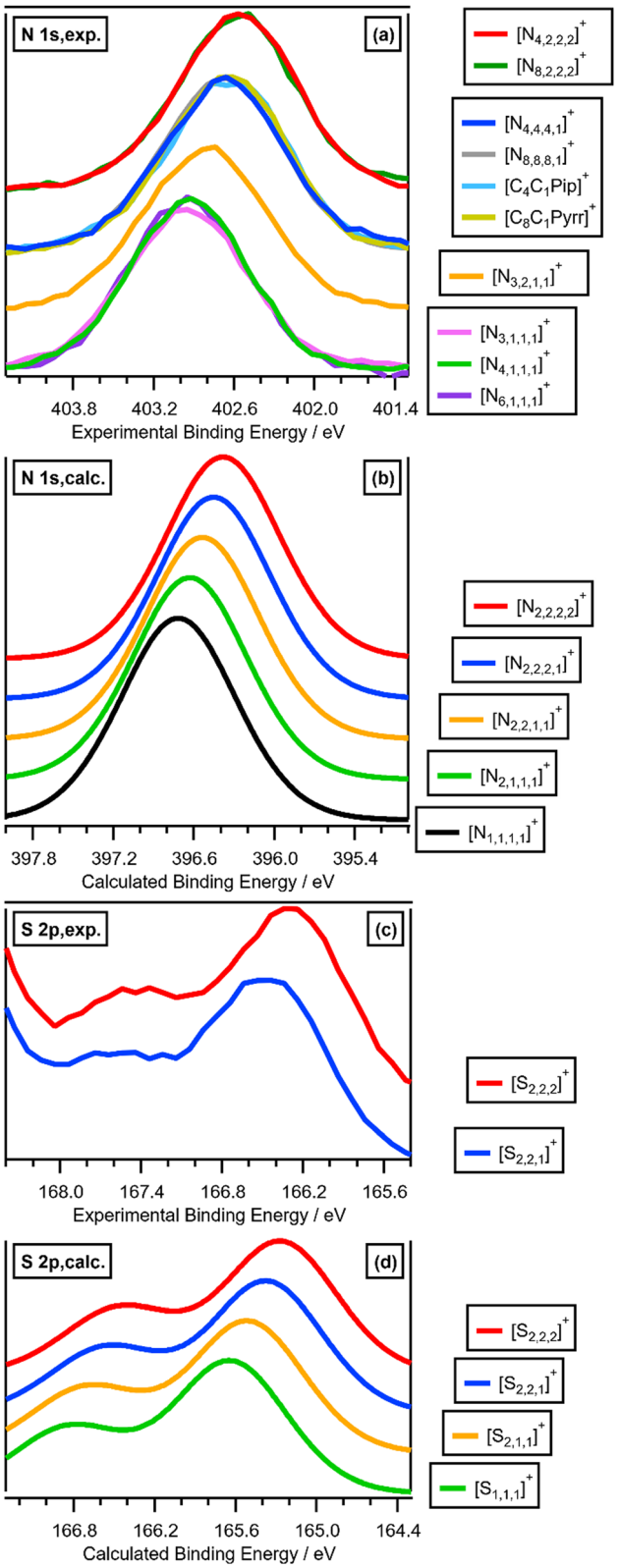

Fig. 2 Experimental and calculated core XP spectra: (a) N 1s,exp. for [cation][NTf_2] where cation = $[N_{3,1,1,1}]^+$, $[N_{4,1,1,1}]^+$, $[N_{6,1,1,1}]^+$, $[N_{3,2,1,1}]^+$, $[N_{4,4,4,1}]^+$, $[N_{8,8,8,1}]^+$, $[C_4C_1Pip]^+$, $[C_8C_1Pyrr]^+$, $[N_{4,2,2,2}]^+$ and $[N_{8,2,2,2}]^+$; (b) N 1s,calc. for $[N_{1,1,1,1}]^+$, $[N_{2,1,1,1}]^+$, $[N_{2,2,1,1}]^+$, $[N_{2,2,2,1}]^+$ and $[N_{2,2,2,2}]^+$; (c) S 2p,exp. for $[S_{2,2,1}][NTf_2]$ and $[S_{2,2,2}][NTf_2]$; (d) S 2p,calc. for $[S_{1,1,1}]^+$, $[S_{2,1,1}]^+$, $[S_{2,2,1}]^+$ and $[S_{2,2,2}]^+$. Experimental XP spectra are area normalised and charge referenced using methods given in ESI,† Section S5. Traces are vertically offset for clarity.

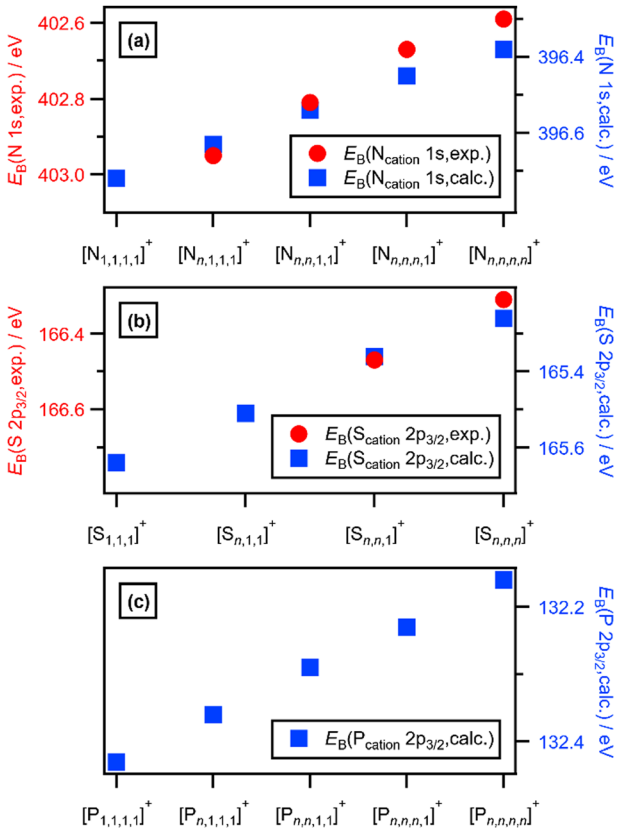

Fig. 3 (a) Experimental and calculated $E_B(N_{cation}\ 1s)$. (b) Experimental and calculated $E_B(S_{cation}\ 2p_{3/2})$. (c) Calculated $E_B(P_{cation}\ 2p_{3/2})$. Where n is used as a label in this figure, $n \geq 2$.

The effect of varying alkyl chain lengths for all key fully alkylated oniums is the same. For $[S_{n,n,n}]^+$ and $[P_{n,n,n,n}]^+$ cations the effect of changing from methyl to longer alkyl substituents on $E_B(S_{cation}\ 2p)$ and $E_B(P_{cation}\ 2p)$ respectively match those of $E_B(N_{cation}\ 1s)$ for $[N_{n,n,n,n}]^+$. Comparing experimental S 2p XPS for the two ILs $[S_{2,2,1}][NTf_2]$ and $[S_{2,2,2}][NTf_2]$ gave $\Delta E_B(S\ 2p_{3/2}) = -0.16$ eV (Fig. 2c and 3b). Furthermore, going from $[S_{2,2,1}]^+$ to $[S_{2,2,2}]^+$, gives a calculated $\Delta E_B(S\ 2p_{3/2}) = -0.10$ eV (Fig. 2c and 3b and ESI,† Table S8), demonstrating that the calculations match the experiments very well. Moreover, for $[P_{n,n,n,n}]^+$ each time a methyl is changed to a longer alkyl gives $\Delta E_B(P_{cation}\ 2p_{3/2}) \sim -0.07$ eV (Fig. 3c and ESI,† Fig. S21).

The excellent matches for the experimental and calculated $E_B(X_{cation}$ core) (where X = N, S or P) demonstrate that the changes in the experimental $E_B(X_{cation}$ core) are due to ground state effects and can be related directly to the molecular electrostatic potential at the central onium atom nucleus, V_X (Fig. 5). The differences in $E_B(X_{cation}$ core) for fully alkylated onium cations are explained by the alkyl group inductive effect, where the additive strength is $-CH_2CH_2CH_3 \approx -C_2H_5 < -CH_3$.[27] Four CH_3 substituents gives the largest $E_B(X_{cation}$ core) = largest V_X = strongest X atom electrostatic interaction. Conversely, four longer alkyl substituents gives the smallest E_B(Ncation 1s) = smallest V_X = weakest X atom electrostatic interaction.

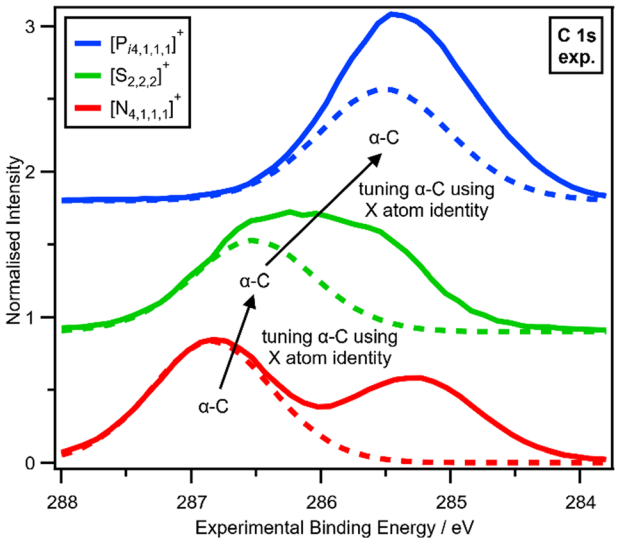

Fig. 4 Tuning α-C using X atom identity. Experimental C 1s XP spectra for $[P_{i4,1,1,1}][NTf_2]$, $[S_{2,2,2}][NTf_2]$ and $[N_{4,1,1,1}][NTf_2]$ ionic liquids. Experimental XP spectra are area normalised and charge referenced using methods given in ESI,† Section S5. Traces are vertically offset for clarity.

Changing the alkyl groups from linear to branched (*i.e.* going from each α-C atom having one C and two H to each α-C atom having two C and one H) gives a small impact on $E_B(N_{cation}\ 1s)$ and V_N. Changing the cation from $[N_{2,2,2,2}]^+$ to $[N_{i3,i3,i3,i3}]^+$ (i3 = isopropyl, ESI,† Table S3) gave $\Delta E_B(N_{cation}\ 1s) = -0.09$ eV (ESI,† Fig. S22 and Table S9). $[N_{i3,i3,i3,i3}]^+$ is unlikely to be stable in solution, but adding one branched alkyl group to give *e.g.* $[N_{i3,2,2,2}]^+$ will give stable cations and will allow fine tuning of $E_B(N_{cation}\ 1s)$ and V_N.

The electronic environment of the carbon atoms in onium cations can be finely controlled by changing X_{cation} (Fig. 4 and ESI,† Section S14), as demonstrated by using our second spectroscopic handle, E_B(C 1s). $E_B(C_{\alpha\text{-}C}\ 1s)$ and therefore V_C can be tuned using the central X atom identity. The experimental order for $E_B(C_{\alpha\text{-}C}\ 1s)$ is N > S > P (Fig. 4), which matches literature E_B for N *versus* P (S was not included in ref. 22), partial charge calculations,[28] and also matches the order of the central atom electronegativity, *i.e.* N > S > P, so nitrogen withdraws the most electron density from α-C to X_{cation} (Fig. 5).

V_X for X_{cation} can be inferred from $E_B(C_{\alpha\text{-}C}\ 1s)$, given that all onium cations will have approximately the same overall charge of +1, so any change in $V_{\alpha\text{-}C}$ will have the opposite effect on V_X. $E_B(C_{\alpha\text{-}C}\ 1s)$ and $V_{\alpha\text{-}C}$ trend N > S > P, so V_X (relative to a neutral X atom) trends P > S > N.

Both $E_B(X_{cation}$ core) and $E_B(C_{\alpha\text{-}C}\ 1s)$ can be tuned using the counteranion identity.[19,21,22] Changing from Cl^- to $[NTf_2]^-$ had the same effect (within experimental uncertainty) of +0.4 eV on $E_B(C_{\alpha\text{-}C}\ 1s)$, $\Delta E_B(N_{cation}\ 1s)$ and $\Delta E_B(P_{cation}\ 2p)$.[19,21,22] This effect of the anion is similar in magnitude to changing from four alkyl substituents to four longer alkyl substituents (Fig. 3).

Given that the onium cation headgroup will dominate any electrostatic interaction with a substrate, both V_X and $V_{\alpha\text{-}C}$ are clearly vital descriptors. We have demonstrated that both V_X and $V_{\alpha\text{-}C}$ can be predictably controlled for onium cations by the

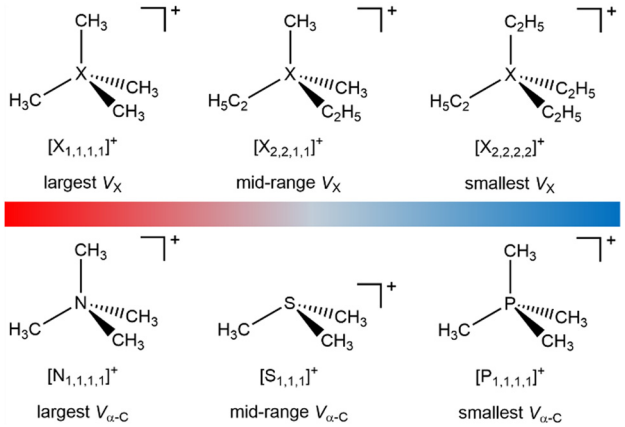

Fig. 5 Effect of the onium cation structure on V_X and $V_{\alpha\text{-}C}$.

choice of alkyl chain length and central X atom identity. Furthermore, for certain applications where cation–anion are likely to be bound together (*e.g.* ion pairing in solvents with low relative permittivity, in ionic liquids), the counteranion identity can also contribute strongly to both V_X and $V_{\alpha\text{-}C}$.

We envisage this information being useful in two areas. Firstly, V_X and $V_{\alpha\text{-}C}$ are expected to be very useful descriptors for developing models using both quantitative structure–property relationships (QSPR) and machine learning. Such descriptors could be calculated using the same DFT methods demonstrated here, or a cheaper but cruder method would be to use the linear relationships developed here to make predictions of V_X and $V_{\alpha\text{-}C}$. Secondly, a semi-quantitative judgement of the optimum onium cation to be used in any application can be made using our results. The largest V_X (*i.e.* strongest X atom electrostatic interaction) would be $[X_{1,1,1,1}][FAP]$ (the very weakly electrostatically interacting anion $[FAP]^-$ = tris(pentafluoroethyl)-trifluorophosphate[19]), and the smallest V_X (*i.e.* weakest X atom electrostatic interaction) would be *e.g.* $[X_{2,2,2,2}]Cl$. For biocides for example, a strong electrostatic interaction is expected to be desirable. Therefore, focusing on electronic effects (and ignoring steric effects) $[X_{1,1,1,1}]^+$ would be better than $[X_{2,2,2,2}]^+$. However, such a selection is challenging as both V_X and $V_{\alpha\text{-}C}$ are affected in opposite directions by the central X atom identity, and a single site interaction model cannot be assumed.

We have presented new experimental and calculated electronic descriptors for judging electrostatic interaction strengths in fully-alkylated onium cations (Fig. 5). X_{cation}, α-C and C_{alkyl} can be predictably tuned using a combination of the alkyl chain lengths, the central X atom identity and the counteranion.

We acknowledge support from the Royal Society for a University Research Fellowship for K. R. J. L. (URF\R\150353 and URF\R\211005) and further awards (RGF\EA\180089, RGF\R1\180053, RF\ERE\210061 and RF\ERE\231015). R. P. M. acknowledges support from the Royal Society of Chemistry through the RSC Research Fund grant (R21-4762139998). We acknowledge Diamond Light Source for time on Beamline B07-B under Proposals SI29413, SI30367, SI31939, SI33378 and SI35207.

Data availability

The data underlying this study are openly available in the University of Reading Research Data Archive at **https://doi.org/10.17864/1947.001349**. Analysed data supporting this article have been included as part of the ESI.†

Conflicts of interest

There are no conflicts to declare.

Notes and references

1 F. Bures, *Top. Curr. Chem.*, 2019, **377**, 14.
2 S. Shirakawa, *et al.*, *Angew. Chem., Int. Ed.*, 2015, **54**, 15767–15770.
3 T. Nakamura, *et al.*, *Chem. – Asian J.*, 2020, **15**, 463–472.
4 O. G. Mancheño and M. Waser, *Eur. J. Org. Chem.*, 2023, 8.
5 S. Mohapatra, *et al.*, *J. Hazard. Mater.*, 2023, **445**, 130393.
6 M. C. Jennings, *et al.*, *ACS Infect. Dis.*, 2015, **1**, 288–303.
7 D. R. MacFarlane, *et al.*, *J. Phys. Chem. B*, 1999, **103**, 4164–4170.
8 F. Mast, *et al.*, *J. Am. Chem. Soc.*, 2024, **146**, 15119–15129.
9 A. E. Somers, *et al.*, *ACS Appl. Mater. Interfaces*, 2013, **5**, 11544–11553.
10 C. Verma, *et al.*, *Adv. Colloid Interface Sci.*, 2022, **306**, 102723.
11 N. M. Mustafa, *et al.*, *Heliyon*, 2024, **10**, e27381.
12 P. Gilbert and L. E. Moore, *J. Appl. Microbiol.*, 2005, **99**, 703–715.
13 D. Kwasniewska, *et al.*, *Pathogens*, 2020, **9**, 459.
14 C. C. Zhou and Y. L. Wang, *Curr. Opin. Colloid Interface Sci.*, 2020, **45**, 28–43.
15 S. P. Denyer, *Int. Biodeterior. Biodegrad.*, 1995, **36**, 227–245.
16 A. F. Zahrt, *et al.*, *Science*, 2019, **363**, eaau5631.
17 J. J. Henle, *et al.*, *J. Am. Chem. Soc.*, 2020, **142**, 11578–11592.
18 E. Gousseva, *et al.*, *J. Phys. Chem. B*, 2022, **126**, 10500–10509.
19 E. Gousseva, *et al.*, *J. Phys. Chem. B*, 2024, **128**, 5030–5043.
20 C. H. Suresh and S. Anila, *Acc. Chem. Res.*, 2023, **56**, 1884–1895.
21 S. Men, *et al.*, *Phys. Chem. Chem. Phys.*, 2011, **13**, 15244–15255.
22 R. K. Blundell and P. Licence, *Phys. Chem. Chem. Phys.*, 2014, **16**, 15278–15288.
23 R. K. Blundell and P. Licence, *Chem. Commun.*, 2014, **50**, 12080–12083.
24 R. M. Fogarty, *et al.*, *Phys. Chem. Chem. Phys.*, 2019, **21**, 18893–18910.
25 J. M. Seymour, *et al.*, *Phys. Chem. Chem. Phys.*, 2021, **23**, 20957–20973.
26 K. R. J. Lovelock, *et al.*, *Chem. Rev.*, 2010, **110**, 5158–5190.
27 R. W. Taft, *et al.*, *J. Am. Chem. Soc.*, 1978, **100**, 7765–7767.
28 L. K. Scarbath-Evers, *et al.*, *Phys. Chem. Chem. Phys.*, 2015, **17**, 20205–20216.